Both phenotypic and genotypic sex influence sex chromosome dosage compensation in a sex reversing lizard

Benjamin J. Hanrahan[1], J King Chang[1], Nicholas C. Lister[1], Duminda S.B. Dissanayake[2], Jillian M. Hammond[3,4], Andre L.M. Reis[3,4,5], Ira W. Deveson[3,4,5], Aurora Ruiz-Herrera[6,7], Hardip R. Patel[8], Jennifer A. Marshall Graves[2,9], Arthur Georges[2], Paul D. Waters[1]

[1] School of Biotechnology and Biomolecular Sciences, Faculty of Science, UNSW Sydney, Sydney, NSW 2052, Australia.

[2] Institute for Applied Ecology, University of Canberra, Canberra, ACT 2601 Australia.

[3] Genomics Pillar, Garvan Institute of Medical Research, Sydney, NSW, Australia.

[4] Centre for Population Genomics, Garvan Institute of Medical Research and Murdoch Children's Research Institute, Australia.

[5] Faculty of Medicine, University of New South Wales, Sydney, NSW, Australia.

[6] Departament de Biologia Cel·lular, Fisiologia i Immunologia, Universitat Autònoma de Barcelona, Cerdanyola del Vallès, 08193, Spain.

[7] Genome Integrity and Instability Group, Institut de Biotecnologia i Biomedicina, Universitat Autònoma de Barcelona, Cerdanyola del Vallès, 08193, Spain.

[8] National Centre for Indigenous Genomics, Australian National University, ACT 2601, Australia.

[9] Department of Environment and Genetics, La Trobe University, Melbourne, Victoria 3068, Australia.

Keywords: sex chromosomes, dosage compensation, *Bassiana duperreyi*

Abstract

Studies of sex chromosome dosage compensation have historically focussed on therian mammals which have a conserved XY sex determination system. In contrast, lizards have sex determination systems that can differ between even closely related species that include XY and ZW systems and thermolabile systems where genetic and temperature interact to various degrees to determine sex. The eastern three-lined skink (*Bassiana duperreyi*) has a differentiated XY sex determination system, in which low temperature incubation during development can cause female to male sex reversal, producing XX males. This provides a unique opportunity to investigate how genotype and phenotype affect dosage compensation. We generated transcriptomes from brain and heart tissue of normal adult males and females, along with brain tissue of sex-reversed XX males. We observed partial dosage compensation between XX females and XY males in both brain and heart, with median gene expression from the X in normal males being 0.7 times that of normal females. Surprisingly, in brain of sex reversed XX males the median X chromosome output did not match that of either normal males or females, but instead was 0.89 times that of the normal XX female level. This suggests that not just genotype, but also sexual phenotype, influences gene dosage of the X chromosome. This has profound implications for our understanding of the evolution of dosage compensation.

Introduction:

Sex chromosome dosage compensation was proposed to have evolved in response to loss of gene function from the mammalian Y chromosome. Gene expression from the single X in males should need to be upregulated to restore ancestral autosomal levels. This X upregulation carried through to females resulting in disproportionately high X expression in XX females (1), and this was countered by X chromosome inactivation (XCI) to silence one X chromosome in the somatic cells of females (2). This classic model of dosage compensation appears to hold true for marsupial mammals, but transcriptional upregulation of the single X appears incomplete in eutherian mammals (3, 4). In monotremes, median gene expression from the X chromosome is increased compared to the autosomes in XY males, as it is for the bird Z in ZW females. However, global X (or Z) transcriptional output is not evenly balanced between the sexes (5).

Mammals and birds have ancient and relatively stable sex chromosomes and sex determination systems. Most mammals have a conserved XY system and birds have a conserved ZW system. In contrast, reptiles display a wide array of sex determination and sex chromosome systems, even in closely related species (6, 7). These organisms exhibit not only XY and ZW genetic sex determination (GSD) systems, but also temperature-dependent sex determination (TSD), whereby the sex of offspring is determined by the temperature at which the egg is incubated during a thermosensitive window. GSD and TSD systems are often observed in closely related lizard species, and some species have a GSD system that can be overridden by temperature to cause sex reversal (8-11).

The few studies of reptile dosage compensation have revealed a variety of non-canonical dosage compensation systems. In snakes, there are reports of partial dosage compensation of the Z chromosome by upregulation of Z-borne genes in females (12, 13). The green anole (*Anolis carolinensis*), a lizard with an XY sex chromosome system, has complete dosage compensation of genes on the linkage group representing the most differentiated region of the X, and incomplete dosage compensation of genes on scaffolds representing newer, less differentiated regions (14). In contrast, the Komodo dragon (*Varanus komodoensis*), which has one of the

oldest ZW sex chromosome systems, shows no evidence of dosage compensation of Z-specific genes (15). Little else is known about dosage compensation in other lizards with different sex chromosome systems.

The scincid lizard *Bassiana duperreyi* (Australian eastern three-lined skink) has a differentiated XY sex chromosome system (16) that is thought to predate skink radiation (17). However, the genetic sex determining switch can be overridden by temperature (8, 9, 11). Reduced incubation temperature of eggs during the thermosensitive period results in sex reversed XX males in the adult population and the natural nests of both captive and wild populations (18, 19). This gives rise to three different genotypic and phenotypic sexes: XX females, XY males and sex reversed XX males. Therefore, *B. duperreyi* provides a unique opportunity not only to examine dosage compensation in a reptile with differentiated sex chromosomes, but to also test if dosage compensation in sex reversed XX males follows genotype or phenotype.

Here we present a chromosome level *B. duperreyi* genome assembly from a male individual, in which we have identified both the X and Y chromosomes. We generated mRNA sequence data from brain and heart tissue of genotypically normal XX females and XY males, and brain tissue of XX male individuals to examine the effect of genotype and phenotype on dosage compensation. In brain and heart of normal XY male and XX female individuals, there was partial dosage compensation, such that the single X of XY males was overexpressed. However, in sex reversed XX males, we observed that median gene expression of the X was higher than in XY males, but lower than XX females, such that the X chromosomes of XX males were underexpressed. This raises the intriguing possibility that sex chromosome dosage compensation is not governed solely by genotype, and that phenotype (sex) plays an unknown role.

Results:

Genome summary

Genome length was 1.485 Gbp, assembled into 5,369 contigs/scaffolds. The six largest scaffolds corresponded to autosome macrochromosomes (288.7 - 75.5 Mbp), with the next eight largest scaffolds representing the microchromosomes (54.7 – 18.1 Mbp) (Figure 1A, Table 1). These chromosome-scale scaffolds comprised 98.5% of the total assembled sequence. BUSCO analysis showed 96.0% complete conserved orthologs in the tetrapod database and 96.6% complete conserved orthologs in the vertebrate database (Table 2).

Table 1. Chromosome size and identity

Scaffold Name	Size (bp)	Chromosome Identity
BASDU_flyeontv1_Contig31	288676622	1
BASDU_flyeontv1_Contig51	258390987	2
BASDU_flyeontv1_Contig32	215829809	3
BASDU_flyeontv1_Contig88	205722031	4
BASDU_flyeontv1_Contig66	107145552	5
BASDU_flyeontv1_Contig53	75523483	6
BASDU_flyeontv1_Contig1241	74033703	X
BASDU_flyeontv1_Contig298	54678650	7
BASDU_flyeontv1_Contig235	50055479	12,13,14
BASDU_flyeontv1_Contig328	39280427	8
BASDU_flyeontv1_Contig38	25948193	9
BASDU_flyeontv1_Contig604	22020833	10
BASDU_flyeontv1_Contig93	21659042	Y
BASDU_flyeontv1_Contig1096	18146980	11

Table 2. BUSCO assessment of the *B. duperreyi* genome

BUSCO Assessment	Total	Complete and single-copy	Complete and duplicated	Fragmented	Missing	Groups searched
tetrapod_odb10	5156	5098 (96.0%)	58 (1.1%)	44 (0.8%)	110 (2.1%)	38
vertebrate_odb10	3290	3240 (96.6%)	50 (1.5%)	32 (1.0%)	32 (0.9%)	67

Two scaffolds were identified as the X and Y chromosomes by BLASTn with known Y specific *B. duperreyi* markers. Read depth analysis of short read Illumina whole

genome sequencing from a male individual confirmed identity of these scaffolds as the X and Y chromosomes (Figure 1B), and revealed the pseudoautosomal region (PAR) boundary location at which read coverage increased compared to X and Y specific regions. The X and Y chromosomes were 71.2 Mbp and 21.7 Mbp, respectively, and shared a small PAR of approximately 2.8Mbp that was assembled onto the X scaffold (Figure 1B). Both the X and Y had more interactions with the autosomes, than macrochromosome to macrochromosome interactions (Figure 1A), contrasting eutherian XY systems that have fewer interactions between sex chromosome and autosomes (20). As expected, microchromosomes interacted with each other more than with the macrochromosomes (21).

Annotation identified a total of 13,979 genes in the genome. Of these, 667 were X-specific genes, sharing extensive homology with chicken chromosome 1 (Figure 1C). A total of 65 genes were annotated on the male specific region of the Y: 42 of these were X/Y shared, with the remaining 23 having no X-borne partner so were Y-specific. A total of 39 genes were annotated in the PAR. The karyotypic difference between the X and Y (16), and the disparity between their gene content, confirmed their differentiation. This suggested that a sex chromosome dosage compensation mechanism should be required to balance the output of X-specific genes in XX females and XY males.

Dosage compensation of the X chromosome

In brain and heart, median gene expression from the autosome scaffolds and PAR was equivalent between XY males and XX females (Figure 2A). However, median X chromosome transcriptional output in XY males was reduced compared to XX females (to 70% in brain and 65% in heart: Mood's median test, $p < 0.0001$).

We next tested if phenotypic sex influenced total transcriptional output from the X versus the autosomes in brain. The ratios of median X specific to autosome gene expression levels within the three genotypic and phenotypic sexes were measured. In XX females there was no significant difference between X and autosomal expression levels. In XX males, expression from the X trended down, but this was not statistically significant. In XY males, median transcriptional output from the X was 72% that of the autosomes (permutation test, $p < 0.0001$) (Figure 2B).

We then compared transcriptional output of the X specific region between the three phenotypic and genotypic sexes. Median gene expression from autosome scaffolds and the PAR of XX females, XY males and sex reversed XX males were equivalent (Figure 2C). As observed for heart and brain above, median gene expression from the X chromosome was significantly lower in normal XY males compared to XX females (down to 69%: Mood's median test, $p < 0.0001$) (Figure 2C). Median gene expression from the X chromosome was also lower in XY males than XX males (down to 77%: Mood's median test, $p < 0.0001$). These ratios are both greater than the 50% expected from the dosage of X chromosomes, implying significant upregulation of the single X in XY males relative to XX females and XX males (Figure 2C).

The most interesting comparison of expression ratio from the X was between sex reversed XX males and normal XX females. Although both have two X chromosomes, transcription from the X was significantly lower in XX sex reversed males (down to 89%: Mood's median test, $p < 0.0001$). This must mean that one or both X chromosomes are downregulated in sex reversed XX males. Thus, sex reversed XX males have a median level of X chromosome gene expression that is not equivalent to either their phenotypic (XY male) or genotypic (XX female) counterparts. This result is not region specific on the X (Figure 2D), nor is it restricted to a subset of genes (Figure 2G); rather, it is chromosome wide.

Discussion:

Therian mammals have conserved sex chromosomes and dosage compensation systems. Part of this dosage compensation system is the transcriptional silencing of one X in the somatic cells of females via the epigenetic process of XCI (2). In XXX human females, two Xs are inactivated (22), and in XXY males one X is silenced, leaving one active X (23, 24). This is a reflection of the counting mechanism of XCI, which results in all but one X being silenced in mammals (25) and is entirely genotype dependent.

In contrast, we demonstrate here that in a lizard transcriptional output of genes on the X chromosome is influenced by phenotypic sex, as well as sex chromosome constitution.

In normal XY male *B. duperreyi* there was partial dosage compensation of the X chromosome (Figure 2C), with median X chromosome gene expression 69% that of XX females. Therefore, the single X chromosome is being over-expressed by a factor of approximately 1.45. This is similar to observations in non-therian mammal vertebrates such as platypus (5). However, it is different from dosage compensation in other lizard species: absence of sex chromosome dosage compensation in the ZW system of the Komodo dragon (15), and a mix of complete and partial dosage compensation present in the green anole depending on the age of the region of the X chromosome (14).

Thus, our observation that *B. duperreyi* has a chromosome-wide partial dosage compensation system documents a third dosage compensation strategy in lizards. This implies that different dosage compensation systems have evolved repeatedly and independently in different lizard lineages, perhaps depending on the dosage compensation requirements of the progenitor autosomes from which the sex chromosome systems evolved. Study of more lizards will elucidate the breadth of reptile sex dosage compensation and highlight different evolutionary strategies.

As well as comparing normal XY males and XX females, we examined X expression in sex reversed XX males. Surprisingly, XX males had lower gene expression from

the X when compared to normal XX females, meaning that the expression per X is less in XX males than in XX females. Per X expression in XX males must also be less than expression from the single X in XY males (Figure 3). Therefore, sex chromosome dosage compensation in *B. duperreyi* is influenced not just by genotype, but also by sexual phenotype. This unexpected result is the first example of an effect of phenotype on sex chromosome dosage compensation, which has been viewed as a response strictly to genotype.

Reduced expression from the X in sex reversed XX males contradicts theories that dosage compensation evolves exclusively in response to genotype, that is to the number of X chromosomes. This is the first evidence that phenotypic sex influences sex chromosome transcriptional output, with profound implications for our understanding of how dosage compensation evolves. The underlying mechanism responsible for the effect of phenotypic sex on X gene expression remains unclear. Our observation suggests that there is down regulation of one or both of the Xs in XX males. This is quite the opposite to upregulation of the single X in XY males (Figure 3).

Evolutionary arguments do not offer a satisfactory explanation of our results. If loss of genes from the degenerating Y was not accompanied by dosage compensation, we would expect expression from the two X chromosomes to be equivalent in XX females and XX sex reversed males. If loss of Y genes was accompanied by upregulation of the single X in XY males (which we observed), and upregulation of both Xs also occurred in XX males, we would expect XX males to have increased expression per X chromosome compared to XX females. Alternatively, should the X chromosomes in XX males have the same output as XX females, then XX males and XX females should be equivalent (Figure 3). None of these scenarios explain why expression from the X chromosome is lower in XX males than in XX females. Clearly X chromosome transcriptional output is not entirely a response to the number of X chromosomes. Therefore, we hypothesize that dosage compensation in *B. duperreyi* is influenced by phenotypic sex.

A possible explanation is that transcriptional output of the X in *B. duperreyi* is tuned to be globally lower in males than in females. This would not violate upregulation of

the single X in XY males in response to loss of genes from the Y, which results in the observed partial sex chromosome dosage compensation. However, if reduced expression from the X is optimal for normal males, then X output might be “capped” in phenotypic males irrespective of the number of X chromosomes. There is no subset of X-borne genes that is under expressed, so our results signify a global change in X expression (Figure 2 D-G). Understanding the epigenetic profile of the X chromosomes in the three genotypic and phenotypic sexes will be critical to deciphering the mechanics of dosage compensation in this model.

Temperature-induced sex reversal in lizards is not unique to *B. duperreyi,* having been observed in several species (8, 10). It is possible that sex reversal in lizards is more widespread than previously believed, as it has been systematically investigated in only a few species (26), and there may be numerous other species whose sex reversal status is yet to be confirmed (see 27, 28, 29). Examining dosage compensation in other sex reversing models will reveal if the influence that phenotypic sex exerts on X (or Z) gene expression is a widespread phenomenon in lizards.

Methods

Sample collection and sexing

In December 2020, samples (eggs) of alpine *B. duperreyi* were collected from the field location within the Brindabella Range (Piccadilly Circus – 1240 m a.s.l., 35°21'42.0"S 148°48'12.5"E) after ensuring that approximately 90% of the development period had passed in natural conditions (9). The eggs were then collected, transported to the University of Canberra, and placed in incubators (LabWit, ZXSDR1090) that maintained 23°C, which produces a balanced sex ratio (9). Details egg collection methods (19) and a description of the alpine study site can be found in (30).

To determine phenotypic sex of the hatchlings, tail bases of 3-to-7-day old hatchlings were squeezed to evert the hemipenes (31) and sex was checked again by hemipene transillumination after 5 weeks (19). Tail snips were collected to determine the genotype of the lizards. Genotypic sex was determined for *B. duperreyi* using polymerase chain reaction (PCR)-based molecular sex tests from extracted DNA collected from tissue samples. DNA purity was determined using a NanoDrop 1000 spectrophotometer (NanoDrop Technologies Inc., Wilmington, DE, USA) and quantified using the Qubit 2.0 Fluorometric Quantitation (Invitrogen, Life technologies, Sydney, N.S.W., Australia). The sex-reversal status was determined for *B. duperreyi* using PCR as described by Dissanayake et al. (16), where the genotypic sex was identified based on Y-specific markers allowing identification of XY males (XYm) and XX males (XXm).

RNA extraction and sequencing

Total RNA was extracted from the brain tissue of five XY males (XYm), five XX females (XXfm), and four XX males (XXm). Tissue extracts were homogenized using T10 Basic ULTRA-TURRAX® Homogenizer (IKA, Staufen im Breisgau, Germany) and extracted using TRIzol reagent following the manufacturer's instructions, purifying with an isopropanol precipitation. Seventy-five bp single-ended reads were generated on the Illumina NextSeq 500 platform at the Ramaciotti Centre for Genomics (UNSW, Sydney, Australlia).

DNA extraction and sequencing for assembly

Genomic DNA was extracted from 13 mg of ethanol-preserved muscle tissue from a male (XY) *B. duperreyi*, using the Circulomics Nanobind tissue kit as per the manufacturer's protocols, including the specified pre-treatment for ethanol removal. Library preparation was performed with 3 µg of DNA as input, using the SQK-LSK109 kit from Oxford Nanopore Technologies and sequenced across two promethION (FLO-PRO002) flow cells, with washes (EXP-WSH004) performed every 24 hours.

Genome assembly

The genome assembly pipeline relied on using a combination of whole-genome sequencing ONT long reads, Illumina short reads and Hi-C reads. Firstly, adapters were removed from Illumina and Hi-C reads using TrimGalore v0.6.6 with default parameters. A primary assembly was generated using Flye v2.8.3 (32) and the ONT long reads, with the following parameters "--trestle --iterations 2". Illumina short reads were aligned to the primary assembly with bwa-mem v0.7.17-r1188 and ONT long reads were aligned with minimap2 v2.24-r1122 (33), and both alignments were used to polish the assembly with hypo v0.5.1. Homologous contigs were identified and removed using Purge Haplotigs v1.1.1 (34). Chromosome-length scaffolding was performed with Hi-C data using Juicer v1.6 (35) to generate a contact matrix of the connections between contigs and 3d-dna v180922 to organise the contigs into larger scaffolds. Gaps in the assembly were filled using PBjelly v15.8.24 (36) with the ONT reads. The final assembly was assessed for completeness using BUSCO and accuracy using Merqury v1.3 (37), by comparing the assembly k-mer spectrum to those found in the Illumina reads.

Annotation

The annotation used in this study was generated using AUGUSTUS v3.4.0 (38) with RNA sequencing data from brain, heart and gonad from male and female individuals. Prior to running AUGUSTUS, a transcriptome assembly and a soft-masked genome assembly were generated with Trinity v2.12.0 (39) and RepeatMasker v4.1.2-p1 (40), respectively. AUGUSTUS parameters were optimised with a training set of 500

genes, including 5 rounds of optimisation with exon and UTR parameters, before gene prediction and stitching. Peptides were inferred from the final annotation using gffread v0.12.7 (41) and blasted against the uniprot database with blast v2.11.0 (42) for gene identification. A github repository of this pipeline can be found at https://github.com/kango2/Annotation.

Y specific sequences (16) in *Bassiana* were blasted against the generated *Bassiana duperreyi* genome assembly with blast v2.11.0 (42).

Read depth analysis

DNA was extracted from muscle samples of the individual animals using the Gentra Puregene Tissue Kit (QIAGEN, Australia), following the manufacturer's protocols with the modifications described below. The volume and reagent amounts were adjusted according to the size of the tissue sample, using three times more reagent than specified in the manufacturer's protocols. Additionally, we made modifications to the DNA precipitation steps outlined in the manufacturer's protocol. The DNA thread was spooled out using a galls rod and submerged in 300ul of 70% ethanol, then air dried for one minute. Subsequently, we used TE buffer for DNA hydration and allowed it to dissolve overnight at room temperature.

Raw read quality of the DNA sequencing was assessed using FastQC v0.11.9 (43) and trimmed accordingly with trimmomatic v0.38 (44). Trimmed reads were aligned to the newly generated *B. duperreyi* genome assembly with subread-align command in subread v2.0.1 (45). Read depth in 20000 bp windows was calculated using the bamCoverage command, from deeptools v3.5.1 (46), for the X and Y scaffolds as well as a representative autosomal scaffold (contig 328). The generated BED files were then used to plot read depth across these scaffolds using the ggplot2 package in R v4.2.1.

Bioinformatics analysis of RNA-seq

Raw read quality of RNA sequencing was assessed using FastQC v0.11.9 (43) and trimmed accordingly with trimmomatic v0.38 (44). Trimmed reads were aligned to the newly generated *B. duperreyi* genome assembly with subread-align function in subread v2.0.1 (45). The subread-featurecount function from subread v2.0.1 (47)

was used to count reads that overlapped genomic features using the settings “-0 -2 -t CDS,five_prime_utr,three_prime_utr”, the remaining settings were left as default. Library size and read counts were normalised by counts per million and RPKM respectively using the edgeR package in R v4.2.1 (48). Gene expression ratios were calculated and plotted with the ggplot2 package. Gene expression values were calculated from the RNA-seq data (hatchling brain tissue) of XX females (n=3), XY males (n=3) and sex reversed XX males (n=3). Normalised expression values were used to create male to female median expression ratios between the three genotypic and phenotypic sexes for each gene. Genes were binned according to their location on an autosome, the PAR, X as total output and X where output is adjusted for X complement. For per X median expression ratios, X expression was halved for the sexes with two X chromosomes (XXf and XXm).

Data availability

All sequence data have been submitted to the NCBI sequence read archive under the BioProject ID PRJNA980841.

References

1. Ohno S. Sex chromosomes and sex-linked genes. Berlin, New York etc.: Springer-Verlag; 1967. x, 192 p. p.
2. Lyon MF. X-chromosome inactivation and developmental patterns in mammals. Biol Rev Camb Philos Soc. 1972;47(1):1-35.
3. Xiong Y, Chen X, Chen Z, Wang X, Shi S, Wang X, et al. RNA sequencing shows no dosage compensation of the active X-chromosome. Nat Genet. 2010;42(12):1043-7.
4. Lin F, Xing K, Zhang J, He X. Expression reduction in mammalian X chromosome evolution refutes Ohno's hypothesis of dosage compensation. Proc Natl Acad Sci U S A. 2012;109(29):11752-7.
5. Julien P, Brawand D, Soumillon M, Necsulea A, Liechti A, Schutz F, et al. Mechanisms and evolutionary patterns of mammalian and avian dosage compensation. PLoS Biol. 2012;10(5):e1001328.
6. Sarre SD, Georges A, Quinn A. The ends of a continuum: genetic and temperature-dependent sex determination in reptiles. Bioessays. 2004;26(6):639-45.
7. Ezaz T, Sarre SD, O'Meally D, Graves JAM, Georges A. Sex chromosome evolution in lizards: independent origins and rapid transitions. Cytogenet Genome Res. 2009;127(2-4):249-60.
8. Quinn AE, Georges A, Sarre SD, Guarino F, Ezaz T, Graves JA. Temperature sex reversal implies sex gene dosage in a reptile. Science. 2007;316(5823):411.
9. Shine R, Elphick MJ, Donnellan S. Co-occurrence of multiple, supposedly incompatible modes of sex determination in a lizard population. Ecol Lett. 2002;5(4):486-9.
10. Holleley CE, O'Meally D, Sarre SD, Graves JAM, Ezaz T, Matsubara K, et al. Sex reversal triggers the rapid transition from genetic to temperature-dependent sex. Nature. 2015;523(7558):79-82.
11. Radder RS, Quinn AE, Georges A, Sarre SD, Shine R. Genetic evidence for co-occurrence of chromosomal and thermal sex-determining systems in a lizard. Biol Lett. 2008;4(2):176-8.
12. Vicoso B, Emerson JJ, Zektser Y, Mahajan S, Bachtrog D. Comparative sex chromosome genomics in snakes: differentiation, evolutionary strata, and lack of global dosage compensation. PLoS Biol. 2013;11(8):e1001643.

13. Schield DR, Card DC, Hales NR, Perry BW, Pasquesi GM, Blackmon H, et al. The origins and evolution of chromosomes, dosage compensation, and mechanisms underlying venom regulation in snakes. Genome Res. 2019;29(4):590-601.
14. Rupp SM, Webster TH, Olney KC, Hutchins ED, Kusumi K, Wilson Sayres MA. Evolution of Dosage Compensation in Anolis carolinensis, a Reptile with XX/XY Chromosomal Sex Determination. Genome Biol Evol. 2017;9(1):231-40.
15. Rovatsos M, Rehak I, Velenský P, Kratochvil L. Shared Ancient Sex Chromosomes in Varanids, Beaded Lizards, and Alligator Lizards. Mol Biol Evol. 2019;36(6):1113-20.
16. Dissanayake DSB, Holleley CE, Hill LK, O'Meally D, Deakin JE, Georges A. Identification of Y chromosome markers in the eastern three-lined skink (Bassiana duperreyi) using in silico whole genome subtraction. BMC Genomics. 2020;21(1):667.
17. Kostmann A, Kratochvil L, Rovatsos M. Poorly differentiated XX/XY sex chromosomes are widely shared across skink radiation. Proc Biol Sci. 2021;288(1943):20202139.
18. Dissanayake DSB, Holleley CE, Deakin JE, Georges A. High elevation increases the risk of Y chromosome loss in Alpine skink populations with sex reversal. Heredity (Edinb). 2021;126(5):805-16.
19. Dissanayake DSB, Holleley CE, Georges A. Effects of natural nest temperatures on sex reversal and sex ratios in an Australian alpine skink. Sci Rep. 2021;11(1):20093.
20. Álvarez-González L, Arias-Sardá C, Montes-Espuña L, Marín-Gual L, Vara C, Lister NC, et al. Principles of 3D chromosome folding and evolutionary genome reshuffling in mammals. Cell Rep. 2022;41(12):111839.
21. Waters PD, Patel HR, Ruiz-Herrera A, Álvarez-González L, Lister NC, Simakov O, et al. Microchromosomes are building blocks of bird, reptile, and mammal chromosomes. Proc Natl Acad Sci U S A. 2021;118(45).
22. Nielsen MM, Trolle C, Vang S, Hornshøj H, Skakkebæk A, Hedegaard J, et al. Epigenetic and transcriptomic consequences of excess X-chromosome material in 47,XXX syndrome-A comparison with Turner syndrome and 46,XX females. Am J Med Genet C Semin Med Genet. 2020;184(2):279-93.

23. Kinjo K, Yoshida T, Kobori Y, Okada H, Suzuki E, Ogata T, et al. Random X chromosome inactivation in patients with Klinefelter syndrome. Mol Cell Pediatr. 2020;7(1):1.
24. Zitzmann M, Bongers R, Werler S, Bogdanova N, Wistuba J, Kliesch S, et al. Gene expression patterns in relation to the clinical phenotype in Klinefelter syndrome. J Clin Endocrinol Metab. 2015;100(3):E518-23.
25. Avner P, Heard E. X-chromosome inactivation: counting, choice and initiation. Nat Rev Genet. 2001;2(1):59-67.
26. Holleley CE, Sarre SD, O'Meally D, Georges A. Sex Reversal in Reptiles: Reproductive Oddity or Powerful Driver of Evolutionary Change? Sex Dev. 2016;10(5-6):279-87.
27. Whiteley SL, Castelli MA, Dissanayake DSB, Holleley CE, Georges A. Temperature-Induced Sex Reversal in Reptiles: Prevalence, Discovery, and Evolutionary Implications. Sex Dev. 2021;15(1-3):148-56.
28. Cornejo-Páramo P, Dissanayake DSB, Lira-Noriega A, Martínez-Pacheco ML, Acosta A, Ramírez-Suástegui C, et al. Viviparous Reptile Regarded to Have Temperature-Dependent Sex Determination Has Old XY Chromosomes. Genome Biol Evol. 2020;12(6):924-30.
29. Van Dyke JU, Thompson MB, Burridge CP, Castelli MA, Clulow S, Dissanayake DSB, et al. Australian lizards are outstanding models for reproductive biology research. Australian Journal of Zoology. 2020;68(4):168-99.
30. Dissanayake DSB, Holleley CE, Sumner J, Melville J, Georges A. Lineage diversity within a widespread endemic Australian skink to better inform conservation in response to regional-scale disturbance. Ecol Evol. 2022;12(3):e8627.
31. Harlow PS. A Harmless Technique for Sexing Hatchling Lizards. Herpetol Rev. 1996;27(2):71-.
32. Kolmogorov M, Yuan J, Lin Y, Pevzner PA. Assembly of long, error-prone reads using repeat graphs. Nat Biotechnol. 2019;37(5):540-6.
33. Li H. Minimap2: pairwise alignment for nucleotide sequences. Bioinformatics. 2018;34(18):3094-100.
34. Roach MJ, Schmidt SA, Borneman AR. Purge Haplotigs: allelic contig reassignment for third-gen diploid genome assemblies. BMC Bioinformatics. 2018;19(1):460.

35. Durand NC, Shamim MS, Machol I, Rao SS, Huntley MH, Lander ES, et al. Juicer Provides a One-Click System for Analyzing Loop-Resolution Hi-C Experiments. Cell Syst. 2016;3(1):95-8.
36. English AC, Richards S, Han Y, Wang M, Vee V, Qu J, et al. Mind the gap: upgrading genomes with Pacific Biosciences RS long-read sequencing technology. PLoS One. 2012;7(11):e47768.
37. Rhie A, Walenz BP, Koren S, Phillippy AM. Merqury: reference-free quality, completeness, and phasing assessment for genome assemblies. Genome Biol. 2020;21(1):245.
38. Stanke M, Diekhans M, Baertsch R, Haussler D. Using native and syntenically mapped cDNA alignments to improve de novo gene finding. Bioinformatics. 2008;24(5):637-44.
39. Grabherr MG, Haas BJ, Yassour M, Levin JZ, Thompson DA, Amit I, et al. Full-length transcriptome assembly from RNA-Seq data without a reference genome. Nat Biotechnol. 2011;29(7):644-52.
40. Smit AFA, Hubley R, Green P. RepeatMasker Open-4.0. 2013-2015.
41. Pertea G, Pertea M. GFF Utilities: GffRead and GffCompare. F1000Res. 2020;9.
42. Camacho C, Coulouris G, Avagyan V, Ma N, Papadopoulos J, Bealer K, et al. BLAST+: architecture and applications. BMC Bioinformatics. 2009;10:421.
43. Andrews S. FastQC: a quality control tool for high throughput sequence data. 2010.
44. Bolger AM, Lohse M, Usadel B. Trimmomatic: a flexible trimmer for Illumina sequence data. Bioinformatics. 2014;30(15):2114-20.
45. Liao Y, Smyth GK, Shi W. The Subread aligner: fast, accurate and scalable read mapping by seed-and-vote. Nucleic Acids Res. 2013;41(10):e108.
46. Ramirez F, Ryan DP, Gruning B, Bhardwaj V, Kilpert F, Richter AS, et al. deepTools2: a next generation web server for deep-sequencing data analysis. Nucleic Acids Res. 2016;44(W1):W160-5.
47. Liao Y, Smyth GK, Shi W. featureCounts: an efficient general purpose program for assigning sequence reads to genomic features. Bioinformatics. 2014;30(7):923-30.

48. Robinson MD, McCarthy DJ, Smyth GK. edgeR: a Bioconductor package for differential expression analysis of digital gene expression data. Bioinformatics. 2010;26(1):139-40.

49. Ramirez F, Bhardwaj V, Arrigoni L, Lam KC, Gruning BA, Villaveces J, et al. High-resolution TADs reveal DNA sequences underlying genome organization in flies. Nat Commun. 2018;9(1):189.

50. Lovell JT, Sreedasyam A, Schranz ME, Wilson M, Carlson JW, Harkess A, et al. GENESPACE tracks regions of interest and gene copy number variation across multiple genomes. Elife. 2022;11.

Figure Legends

Figure 1. Genome summary of the *Bassiana duperreyi* assembly

A) Hi-C contact map generated with HiC explorer (49) showing scaffold (chromosome) boundaries. Inset: magnified view of the HiC contact map for microchromosomes with size 18.1 – 55.4 Mb, and the sex chromosomes. Number of contacts are between 100 kbp bins. Below: mean inter-chromosomal interactions for 100 kbp windows between each chromosome. **B)** Number of reads mapped in 20kb windows of male Illumina genome sequencing on a representative autosome (contig 31), the putative Y (contig 93) and X contigs (contig 1241). Vertical red line is the PAR boundary on the X contig. **C)** Synteny across chicken, bassiana and blue tailed skink (*Cryptoblepharus egeriae*) genomes, generated with GENESPACE (50). The bassiana Y scaffold (contig 93, not shown) does not share synteny with the other two species.

Figure 2. Dosage of gene expression between sexes

A) Median expression male (XY) to female (XX) ratios were calculated for brain and heart tissue (n=1 for both). A ratio above zero indicates higher expression in male and a ratio below zero indicates higher expression in female. Median is plotted in the box with exact value above each median. Boxes represent the middle 50% of the data, and whiskers represent 1.5 times the interquartile range. Outliers not plotted. **B)** Brain transcriptomes were used to calculate median RPKM for each sex condition (XYm, XXm and XXf) and plotted for autosomal, X specific and PAR genes as a ratio to autosomal median. Ratio to the autosomal median is plotted in the box with exact value above each median. Permutation tests were used to calculate whether median PAR and X specific RPKMs were statistically different from the median autosome RPKM, as well as if the median PAR RPKM was different from the median X specific RPKM (**** $p<0.0001$, *** $p<0.001$, * $p<0.05$). **C)** Median expression ratios were calculated for pairwise comparisons of the three sexes (XYm, XXm and XXf). Genomic regions were separated and plotted as follows; autosomes (green), PAR (blue), total X output (red) and X output adjusted per X (yellow). Mood's median tests were used to calculate if the ratios for the autosomes and X, as well as Xs between sexes, were statistically different (**** $p<0.0001$). **D)** Expression ratios were calculated for each gene in the X specific region and PAR in a pairwise fashion for

the three sexes. Ratios plotted on a log2 scale and median values are plotted as a line in red for X the specific region and blue for the PAR. **E-G)** Scatterplot of counts per million (CPM) for each gene for each pairwise comparison of **E)** XXf to XYm, **F)** XXm to XYm and **G)** XXf to XXm. X genes are plotted in black with slope plotted as a red line. Autosomal genes are plotted in blue with slope as a green line. Slope and R-squared of each trendline is shown above each plot.

Figure 3. Expected and observed dosage of the X chromosome in sex reversed XX males. Left: The X chromosome must be upregulated to in XY males to reach ~70% of the total X chromosome transcriptional output in females. Centre: Should dosage compensation depend on genotype, then transcriptional output of the X chromosomes in XX males should be the same as XX females (top). Alternatively, if transcriptional output of the X chromosome depends on phenotype, then both X chromosomes should be up regulated (bottom) resulting in total X output greater than that of XX females. Right: The total transcriptional output from X genes in XX males lay between that of XX females and XY male. This could result from an upregulated X (as in XY males) that is coupled with a mostly down-regulated X (top). Alternatively, two partially down-regulated Xs (bottom) could achieve the same transcriptional output.

Supplementary Figure 1. Expression ratios for each autosomal scaffold for the three pairwise sex/ genotype comparisons. Number of genes (n) is show in the key for each contig.

Supplementary Figure 2. Expression ratios were calculated for each gene on a representative autosome in a pairwise fashion for each sex (XYm, XXm and XXf). Values are plotted on a log2 scale and median values for each comparison are plotted as a red line.

Acknowledgements

Sequencing costs for this project were met by grants from Bioplatforms Australia (AusARG initiative) and the Australian Research Council (DP170101147). We acknowledge the Garvan Sequencing Platform.

Funding

P.D.W. and J.A.M. are supported by Australian Research Council Discovery Projects (DP170101147, DP180100931, DP210103512 and DP220101429). P.D.W. and H.R.P. are supported by an NHMRC Ideas Grant (2021172). A.R.-H. acknowledges the Spanish Ministry of Science and Innovation (PID2020-112557GB-I00) and the Agència de Gestió d'Ajuts Universitaris i de Recerca, AGAUR (2021SGR00122).

Competing interests

The authors declare that they have no competing interests.

Ethics approval

Experimentation using animals was approved by the University of Canberra Animal Ethics Committee (AEC 17–26) and NSW (SL102002) and ACT (LT201826, LT2017956) governments granted research permits. Husbandry practices fulfil the Australian Code for the Care and Use of Animals for Scientific Purposes 8th edition (2013) sections 3.2.13–3.2.2.

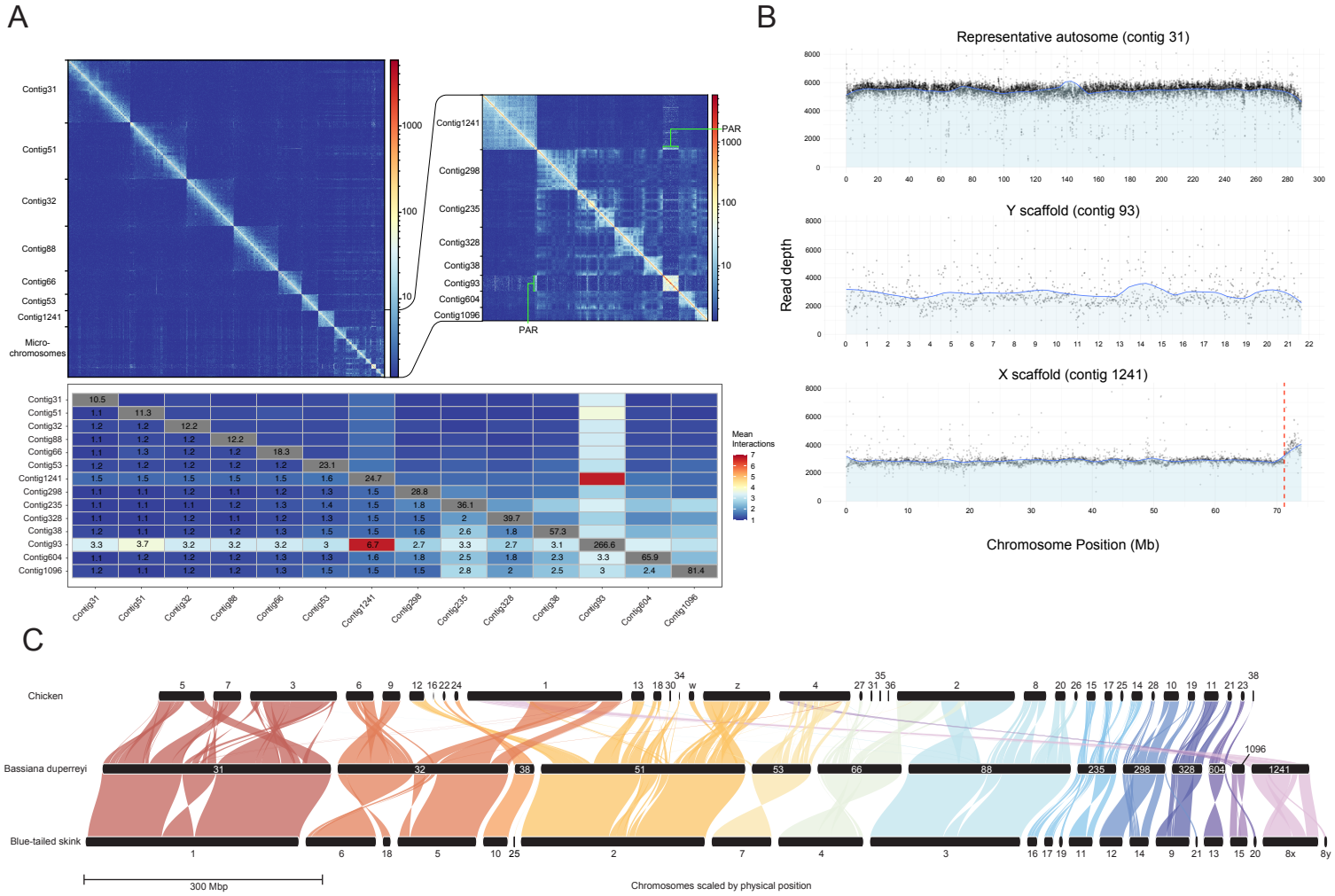
A
Contig31
Contig51
Contig32
Contig88
Contig66
Contig53
Contig1241
Micro-chromosomes
1000
100
10
Contig1241
Contig298
Contig235
Contig328
Contig38
Contig93
Contig604
Contig1096
PAR
PAR
1000
100
10
Mean Interactions
B
Representative autosome (contig 31)
Y scaffold (contig 93)
X scaffold (contig 1241)
Read depth
Chromosome Position (Mb)
C
Chicken
Bassiana duperreyi
Blue-tailed skink
300 Mbp
Chromosomes scaled by physical position

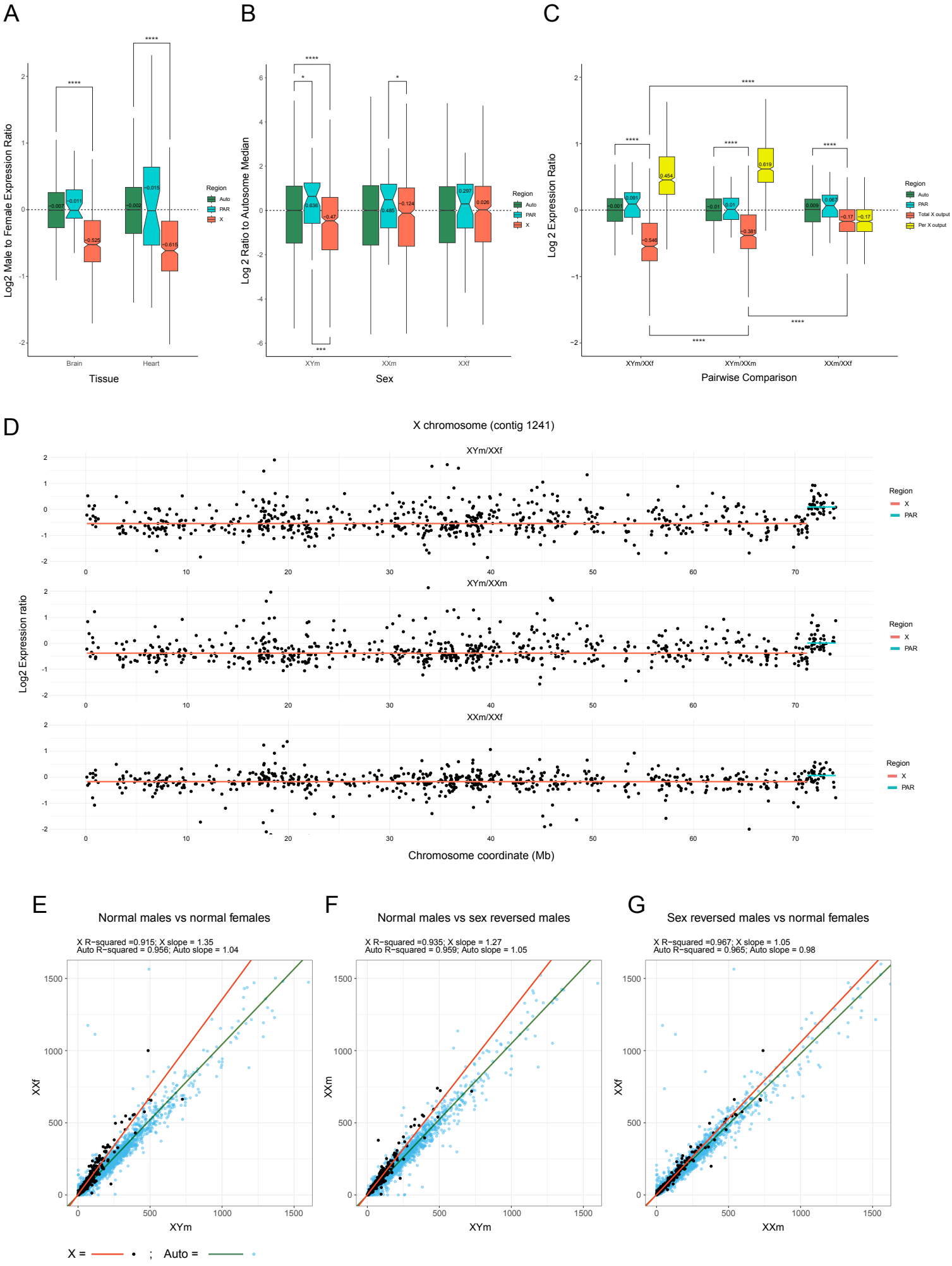
A
Log2 Male to Female Expression Ratio
Brain
Heart
Tissue
Region
Auto
PAR
X
B
Log 2 Ratio to Autosome Median
XYm
XXm
XXf
Sex
C
Log 2 Expression Ratio
XYm/XXf
XYm/XXm
XXm/XXf
Pairwise Comparison
Total X output
Per X output
D
X chromosome (contig 1241)
Log2 Expression ratio
Chromosome coordinate (Mb)
E
Normal males vs normal females
X R−squared =0.915; X slope = 1.35
Auto R−squared = 0.956; Auto slope = 1.04
F
Normal males vs sex reversed males
X R−squared =0.935; X slope = 1.27
Auto R−squared = 0.959; Auto slope = 1.05
G
Sex reversed males vs normal females
X R−squared =0.967; X slope = 1.05
Auto R−squared = 0.965; Auto slope = 0.98
X =
Auto =

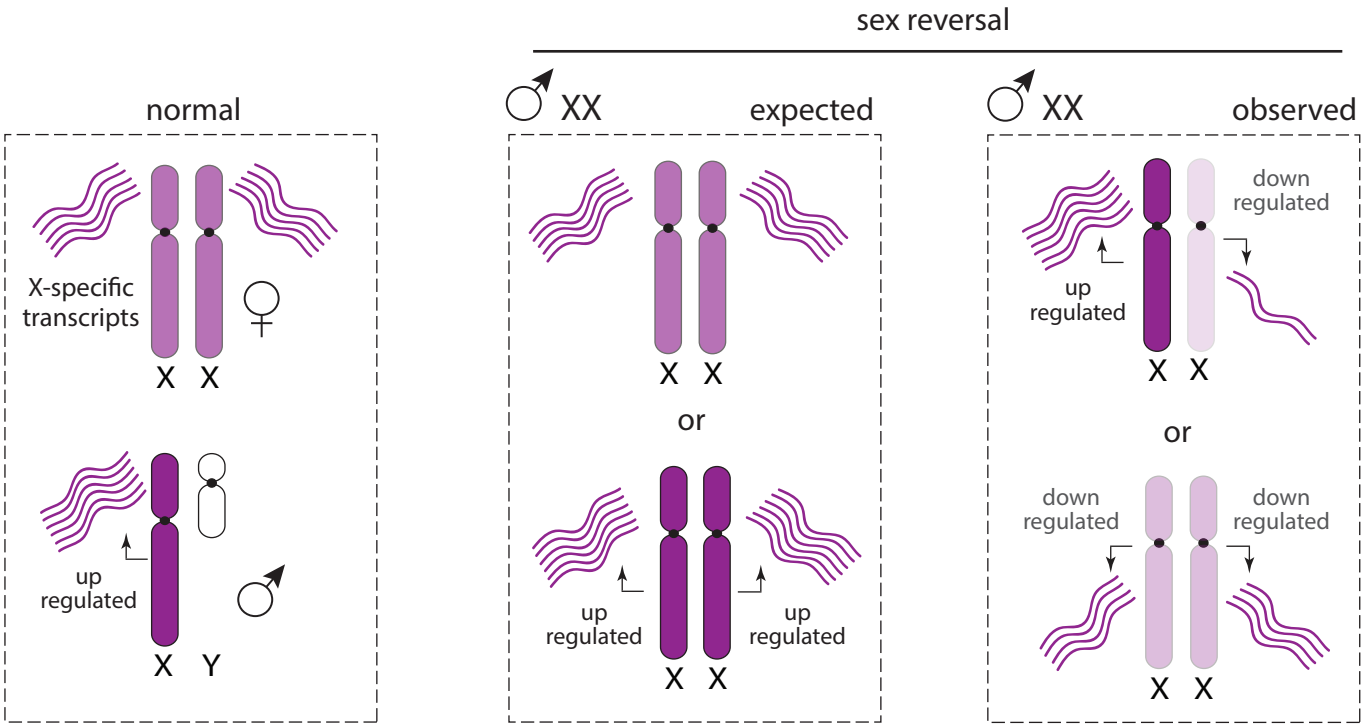
sex reversal
normal
X-specific transcripts
X X
up regulated
X Y
XX
expected
X X
or
up regulated
up regulated
X X
XX
observed
down regulated
up regulated
X X
or
down regulated
down regulated
X X